Research Journal of Applied Sciences, Engineering and Technology 13(11): 835-842, 2016
DOI:10.19026/rjaset.13.3425
ISSN: 2040-7459; e-ISSN: 2040-7467

Submitted: August 23, 2016 Accepted: October 12, 2016 Published: December 05, 2016

Research Article

Study of Residual Stress Relaxation Mechanics Using a Micro-indent Method

[1]F.V. Díaz, [1]C.A. Mammana and [2]A.P.M. Guidobono
[1]Departamento de Ingeniería Electromecánica-Departamento de Ingeniería Industrial, Facultad Regional Rafaela, Universidad Tecnológica Nacional, Acuña 49, 2300 Rafaela, Argentina
[2]División Metrología Dimensional, Centro Regional Rosario (INTI), Ocampo y Esmeralda, 2000 Rosario, Argentina

Abstract: The aim of this study is to show the feasibility and accuracy of a micro-indent method to comprehensively evaluate the relaxation mechanics of residual stress in specimens of rolled aluminium alloy. This micro-indent method was adapted to implement four annealing treatments. The residual displacements were measured using a high-accuracy measuring machine, which enables to decrease the absolute error down to ±300 nm. This study presents an innovative data analysis using Mohr's circles, which allowed to study all directions of the in-plane residual stress for different relaxation times. The results revealed that the relaxation process finishes when the residual stress relief is completed in some preferential directions and then, a brief stress recovery phase begins.

Keywords: Aluminium alloy, micro-indentation, Mohr's circle, relaxation mechanics, residual stresses

INTRODUCTION

Numerous structural or machine component failures result not from stresses due to applied loads but from residual stresses. These stresses are the ones that remain in a component when the external forces and/or moments are zero. Residual stresses are developed when the material undergoes inhomogeneous plastic deformation and/or is exposed to a non-uniform temperature distribution (Withers and Bhadeshia, 2001; Lu, 1996). Difficulty in determining them non-destructively, the unpredictability of their magnitude and direction, their adverse ability to combine with corrosion and fatigue situations and difficulty in removing them can render residual stresses to be extremely troublesome.

The techniques used for residual stress determination can be classified as direct or indirect. The direct techniques consist of determining the residual stress components from the measurement of different physical properties, which are altered by the introduction of these stresses. On the other hand, the indirect methods require breaking the equilibrium of forces and/or moments, which can be obtained by implementing a cutting or the removal of any part of the material evaluated. Among the direct methods, X-ray diffraction has been the most used technique to determine residual stresses (Noyan and Cohen, 1987; Prevéy, 1986). Regarding indirect methods, the most common approach has been the hole-drilling method (Rendler and Vigness, 1966; Gupta, 1973; Díaz *et al*., 2001).

In recent decades, different methods have been developed in order to determine residual stresses through data generated by micro or nano-indentation. Most of these methods compare the contact depth or load-displacement curve of stressed and unstressed specimens, from which the residual stress components can be estimated (Suresh and Giannakopoulos, 1998; Dean *et al*., 2011). Recently, an approach based on the change in distance between micro-indent pairs was developed (Wyatt and Berry, 2006). This change occurs when the residual stresses are relaxed through a thermal treatment. This method has the great advantage of being simple and inexpensive because it does not need specific equipment. More recently, this micro-indent method was improved by using a universal measuring machine (Díaz *et al*., 2010). This improvement allowed evaluating with high precision residual stress distributions generated by high speed milling. It is important to note that for measuring residual displacements this approach only requires a measuring machine and an oven, which are commonly available in many workshops.

Corresponding Author: F.V. Díaz, Departamento de Ingeniería Electromecánica-Departamento de Ingeniería Industrial, Facultad Regional Rafaela, Universidad Tecnológica Nacional, Acuña 49, 2300 Rafaela, Argentina, Tel.: +54 3492 432710; Fax: +54 3492 422880

As it is known, residual stresses can reduce fatigue strength and also may induce stress-corrosion cracking. These difficulties can occur from tensile normal components. On the contrary, compressive normal components can be considered as beneficial because they generate an increase in the fatigue life (Benedetti *et al*., 2010). This improvement is generally caused by an increment in the strength against crack initiation and besides, it can also be caused by the rising in strength against crack propagation (Hearn, 1997). In addition, compressive normal components can introduce beneficial effects on stress-corrosion cracking (Van Boven *et al*., 2007). However, these compressive components could significantly relax under thermal and/or mechanical loadings (Juijerm *et al*., 2007; Luan *et al*., 2009).

The purpose of this study is to demonstrate the feasibility of a high-accuracy micro-indent method for evaluating the relaxation mechanics of compressive components of residual stress in AA 6082-T6 aluminium alloy specimens subjected to thermal loadings. In the present implementation of the method, four annealing treatments were performed in order to evaluate the relaxation mechanics at different times. The sensitivity of the method was evaluated through weak residual stress fields. The residual displacements were measured using a high precision measuring machine, which allowed reducing the absolute error of measurement down to ±300 nm. The residual stresses were calculated from the residual displacements using a model for the plane stress state. In this study, the relaxation process was studied in all directions in the in-plane residual stress field. It must be noted that similar studies have not been found in the literature. The results show that the relaxation of the normal components of residual stress is a linear function of time for all directions of the in-plane residual stress field. A detailed analysis of normal and tangential components of residual stress was performed using a graphical tool known as Mohr's circle (Gere, 2001). Through this tool, it was detected that the relaxation process finishes when the relief is completed in some preferential directions and immediately, a residual stress recovery process is activated. Finally, the values of residual stress obtained at the end of the recovery process reveal that the final state of the relaxed compressive components is quasi-isotropic.

MATERIALS AND METHODS

This study was carried out in the year 2016 at the Departamento Ingeniería Electromecánica, Facultad Regional Rafaela, Universidad Tecnológica Nacional.

The experimental investigations were performed from a hot-rolled sheet of AA 6082-T6 aluminium alloy. The thickness of this rolled sheet is 4 mm. Due to an optimized distribution of precipitate particles of $AlMg_2$ in the aluminium matrix (Tiryakioğlu and Staley, 2003), this alloy has the higher mechanical strength of the 6000 aluminium alloy series. It must be noted that AA 6082-T6 is a relatively new alloy, which is used for structural applications in the marine and transportation industries as well as for machined precision parts in the automotive industry.

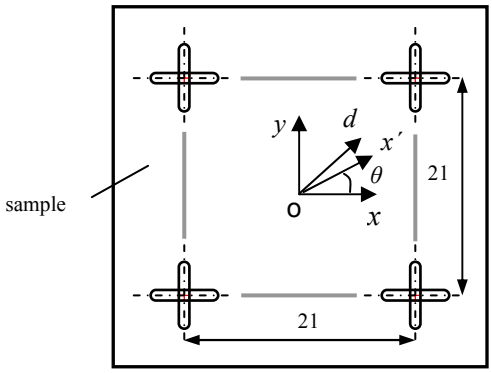

Fig. 1: Distribution of micro-indents

The measured samples were rectangular cross-section plates of 30×30×4 mm. The measurement method consisted of two steps. First, a micro-indent distribution was introduced in each surface evaluated. Then, the micro-indent coordinates were optically measured, before and after a thermal treatment, using a high precision measuring machine (GSIP MU-314). For studying the residual stress relaxation mechanics in function of time, four samples were evaluated. The thermal treatments corresponding to the second step of the method consisted of holding the samples at 300°C for 20, 60, 80 and 100 min.

All components of the in-plane residual stress can be obtained from the micro-indent coordinates. It must be noted that for measuring the through-thickness residual stress distribution, a progressive removal of uniform layers from the specimen surface by chemical etching is needed. However, if out-of-plane direction is considered, residual stresses are usually difficult to measure in thin layers of affected material, even by highly sophisticated techniques like neutron diffraction (Allen *et al*., 1985).

In this study, a special design device was used to attain greater accuracy in both micro-indent introduction and coordinate measurements. This device is attached to the main spindle of the measuring machine (Díaz *et al*., 2010). The body of the device is made up of a system of thin elastic sheets that enables to regulate the indentation load. In addition, an electronic sensor allows calibrating the depth of indent with high accuracy. By using this device, it is possible to introduce different types of micro-indents. In this study, elongated micro-indents were introduced in order to reduce the uncertainty associated with the referencing and measuring processes (Farago and Curtis, 1994). Figure 1 shows the distribution of eight micro-indents introduced in each specimen. From this

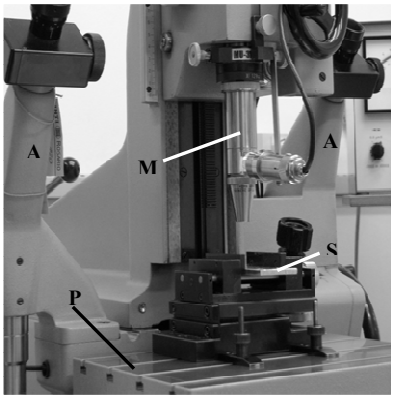

Fig. 2: Picture of the measuring machine: M: main microscope; A: auxiliary microscopes; S: specimen; P: precision stage

distribution, all directions of the in-plane residual stress field can be evaluated in the barycenter of the square generated. It is noteworthy that local residual stress fields are introduced by indentation. However, the errors generated by those fields can be minimized by a proper separation of the micro-indents evaluated. In our case, the nominal distance was 21 mm (square side).

Figure 2 shows the main and auxiliary microscopes used for measuring the micro-indent coordinates. It is noteworthy that the main microscope is a high precision accessory of a measuring machine (Busch *et al*., 1998). Figure 2 also shows a sample, which is positioned on a high precision stage. The micro-indent positions were strictly defined with respect to the optical axis of the main microscope. This axis is orthogonal to the staging plane, which contains two perpendicular displacement axes. The micro-indents were localized by high precision stage displacements. In the measuring machine used in this study (GSIP MU-314), the displacement ranges are 400 mm (longitudinal axis) and 100 mm (transversal axis). It is important to note that the micro-indent coordinates were measured using the main and auxiliary microscopes with accuracy better than 100 nm. Furthermore, nominal distances of 21 mm were determined in both orthogonal axes and the absolute error associated to these distances was evaluated taking into account both nominal and statistical measurement errors. The absolute error obtained from these nominal distances was ±200 nm.

The measurement of micro-indent coordinates was performed within a temperature range of 20±0.2°C, with a variation less than 0.01°C/min. It is important to mention that if this variation is higher than the aforementioned value, the measurement error will significantly increase.

RESIDUAL STRESS DETERMINATION

For determining all components of the in-plane residual strain, normal components in three directions are calculated from the micro-indent coordinates measured. Two of these directions correspond to the reference axes x and y. The other direction, d in Fig. 1, is the bisector of those orthogonal directions. The strain components can be expressed as

$$\varepsilon_x = \frac{l_x - l'_x}{l'_x} \quad \varepsilon_y = \frac{l_y - l'_y}{l'_y} \quad \varepsilon_d = \frac{l_d - l'_d}{l'_d} \tag{1}$$

where: l_x and l'_x are the mean values of the horizontal sides of the square of Fig. 1, l_y and l'_y are the mean values of the vertical sides, in both cases before and after the corresponding thermal treatment, respectively. In addition, l_d and l'_d are the positive slope diagonal of the square, also before and after the thermal treatment, respectively. Then, the angular component of the in-plane residual strain can be obtained

$$\gamma_{xy} = 2 \cdot \varepsilon_d - \varepsilon_x - \varepsilon_y \tag{2}$$

Furthermore, the in-plane strain components associated to an arbitrary direction x' can be expressed as (Timoshenko and Goodier, 1970):

$$\begin{aligned} \varepsilon_{x'} &= \frac{\varepsilon_x + \varepsilon_y}{2} + \frac{\varepsilon_x - \varepsilon_y}{2}\cos 2\theta + \frac{\gamma_{xy}}{2}\sin 2\theta \\ \gamma_{x'y'} &= (\varepsilon_y - \varepsilon_x)\cdot \sin 2\theta + \gamma_{xy} \cdot \cos 2\theta \end{aligned} \tag{3}$$

where, θ is the angle between the arbitrary direction x' and the reference axis x (Fig. 1). Finally, the shear component can be expressed as (Gere, 2001):

$$\varepsilon_{x'y'} = \gamma_{x'y'} / 2 \tag{4}$$

Although for obtaining the relaxed values of residual stress the specimens were treated at 300°C for 20, 60, 80 and 100 min, effects of plasticity and creep strains (inelastic strains) can be considered negligible because very low macro-stresses are evaluated and besides, the holding times are not excessive (Bruin, 1982; Seifi and Salimi-Majd, 2012). It is important to note that the dominant deformation mechanism for that temperature and very low stresses is bulk diffusion through the lattice (Nabarro-Herring creep) (Schoeck, 1961; Ashby, 1972). In addition, thermal components also can be considered negligible because the specimen geometry is simple, the thickness is small and the cooling rate of the different thermal treatments is slow (Das and Chandra, 2003). Therefore, considering the studied material as homogeneous, isotropic and linearly elastic and assuming a plane stress state on the surface of each specimen, the in-plane residual stress components σ_x, σ_y and τ_{xy} can be obtained from Eq. (1) and (2) (Gere, 2001). Then, the normal and tangential components associated to an arbitrary direction x' can be obtained through (Timoshenko and Goodier, 1970):

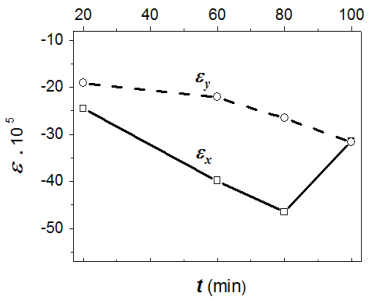

Fig. 3: Variation of the strain components

$$\sigma_{x'} = \frac{\sigma_x + \sigma_y}{2} + \frac{\sigma_x - \sigma_y}{2}\cos 2\theta + \tau_{xy} \cdot \sin 2\theta$$
$$\tau_{x'y'} = -\frac{\sigma_x - \sigma_y}{2}\sin 2\theta + \tau_{xy} \cdot \cos 2\theta \quad (5)$$

Finally, by using the probable absolute error equation (Bevington and Robinson, 2003), the absolute errors associated with the displacement, strain and stress components were obtained from the absolute error corresponding to the nominal distance between micro-indents (±200 nm). The error ranges obtained were ±300 nm, ±0.001% and ±0.9 MPa, respectively.

RESULTS AND DISCUSSION

Figure 3 shows the normal components of residual strain in the directions x and y. The values are compressive. It is important to note that the measured strains are positive (the release of negative residual stresses generates positive strains). The behavior of the ε_x component is linear between 20 and 80 min. Therefore, the strain rate is constant during this interval. After 80 min, the strain direction changes. On the other hand, the ε_y component has the same direction in the complete interval. Furthermore, the strain rate increases slightly after 60 min. Although in both directions (x and y) the strain processes are different, the strain values for 100 min are very similar.

Figure 4a shows the residual stress components associated to ε_x and ε_y. It must be noted that the values of both components (σ_x and σ_y) represent the magnitudes relaxed at the corresponding time. These components are also compressive. From 20 to 80 min both functions are linear, but with different slopes. This fact implies different relaxation rates. After 80 min, the σ_y component is constant and the σ_x component decreases in absolute value. The values for 100 min are also very similar.

The normal components σ_p and σ_q, which correspond to the principal directions, are shown in Fig. 4b. It should be noted that the principal directions are those associated with the normal components whose values are maximum and minimum (Gere, 2001). In this case, σ_p and σ_q correspond to the more and less compressive components, respectively. The results

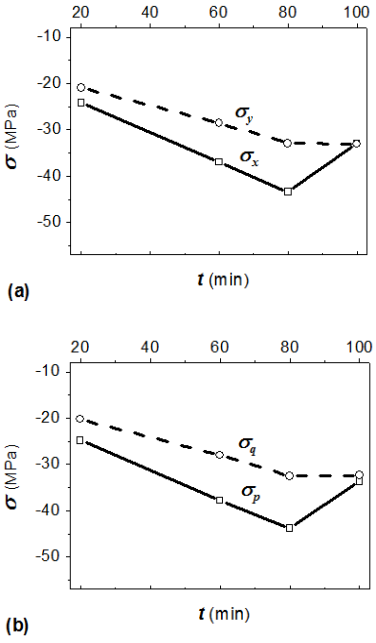

Fig. 4: Stress components variation associated with the (a) reference and (b) principal axes

obtained for both components are very similar to those corresponding to σ_x and σ_y. Therefore, the principal directions will be very close to the reference axes x and y.

Figure 5 shows the Mohr's circles obtained for each time evaluated. It is important to note that, in each circle, the orthogonal coordinates of each point correspond to the normal (abscissa) and tangential (ordinate) components associated with a direction rotated an angle θ with respect to the reference axis x (Fig. 1). Therefore, each circle contains information about normal and tangential components in all in-plane directions. Each circle includes a small segment which defines the point corresponding to the reference direction (θ = 0 in Fig. 1). The residual strain circles corresponding to each evaluated time are shown in Fig. 5a. In each circle, all normal components are compressive. The change from 20 to 80 min implies circle shifting to left and also increase in diameter. This means that the normal components increase in absolute value in all in-plane directions. The circle corresponding to 100 min has very small diameter, which means that the normal components are very similar in all directions (quasi-isotropic state).

Figure 5b shows the Mohr's circles corresponding to the residual stresses relaxed. In these circles, an important difference between the values of the normal and tangential components is observed. Although the distribution of strain and stress circles is similar, the stress circles are more away from each other, which means that the stress states are more independent than the strain states. As expected, the change from 80 to 100 min implies a drastic reduction in diameter and also

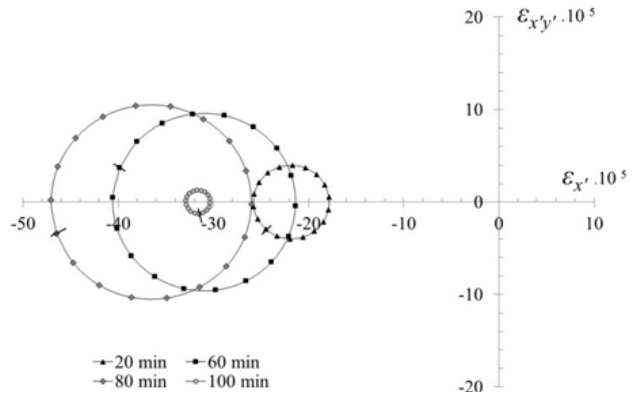

(a)

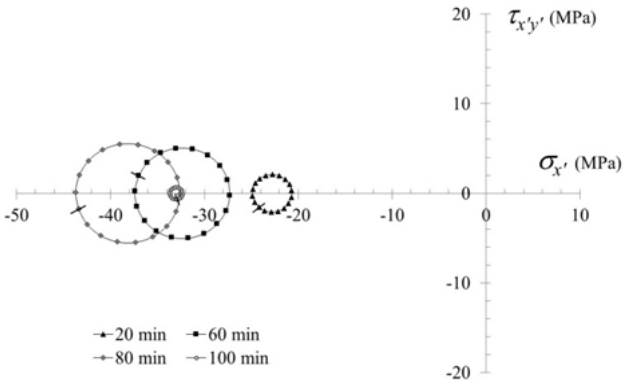

(b)

Fig. 5: (a) Strain and (b) stress Mohr's circles

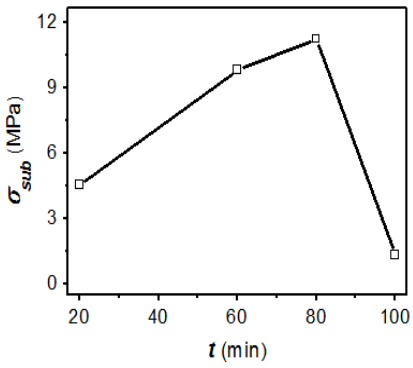

Fig. 6: Variation of the subtraction of principal components

a shifting to right. In addition, both circles share the abscissa corresponding to the less compressive principal component σ_q.

The anisotropy degree of the relaxed, normal components can be evaluated from the subtraction of the principal components

$$\sigma_{sub} = \left|\sigma_p - \sigma_q\right| \quad (6)$$

It must be noted that σ_{sub} corresponds to the diameter of Mohr's circle. The variation of σ_{sub} in function of time is shown in Fig. 6. Between 20 and 80 min, the increase of the variable is quasi-linear. After 80 min this diminishes rapidly approaching to zero. Figure 7 shows the directions associated to the more compressive principal component σ_p. These directions were obtained by evaluating each Mohr's circle. The results obtained from 20 to 80 min show that the final location of the principal directions would respond to the influence of the rolling direction. It is noteworthy that these results corroborate those obtained from cutting operations after rolling, where the behavior of AA 7075-T6 aluminium alloy was evaluated (Díaz *et al*., 2015). However, the principal direction corresponding to 100 min, departs from the rolling direction.

The variation of the mean normal component σ_m is shown in Fig. 8. This normal component is the most representative of all in-plane directions because its value is the abscissa of the center of the Mohr's circle (Gere, 2001). As expected, the behavior is linear between 20 and 80 min. In this time span, the variation

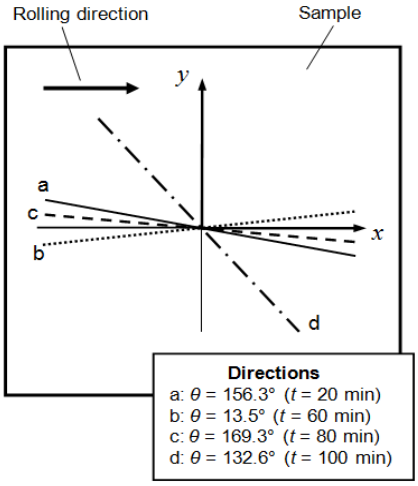

Fig. 7: Variation of the more compressive principal direction

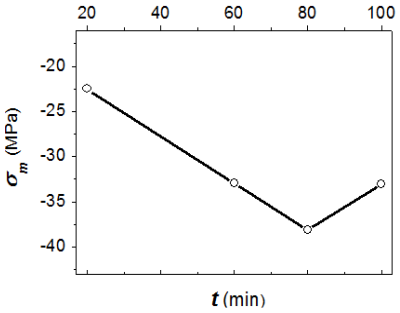

Fig. 8: Variation of the mean stress component

of different normal components of residual stress is linear regardless of the direction evaluated (Fig. 4). Furthermore, as above mentioned, the principal stress subtraction, which represents the anisotropy degree of the normal components, is quasi-linear in that interval and besides, the principal directions are close to the rolling direction.

Taking into account the results showed in Fig. 5b, from 20 to 80 min the relaxation process of residual stress develops relieving compressive normal components in all directions. The relief of these components is linear in time. In addition, in the same time span, the relaxation process also progresses relieving tangential components in all directions. On the other hand, Fig. 4 and 6 show that from 80 min there is a change of sign in the slopes of both the normal components and stress subtraction. This reveals a significant modification in terms of stress relaxation mechanics. In fact, at 80 min the stress subtraction (anisotropy degree) is maximized, which means that the relieved tangential components are maximized (Gere, 2001). On the contrary, as is shown in the smallest Mohr's circle in Fig. 5b, the tangential components associated with the stress relaxation at 100 min are extremely small. It is noteworthy that the ratio of the maximum tangential component values at 80 and 100 min is approximately 8.

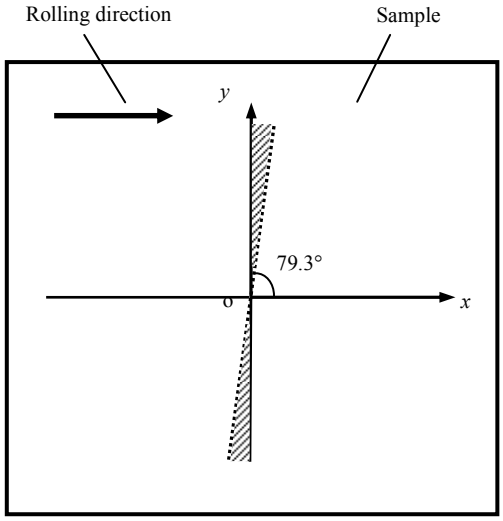

Fig. 9: Directions relaxed completely at 80 min

If the normal components ε_x and ε_y are evaluated from 80 to 100 min (Fig. 3), they have opposite directions and its ratio is 0.33, which is the Poisson's ratio of the material. In this time span, small residual stresses associated with these strains are retrieved in the x direction. This is revealed in Fig. 4a, where the relaxation of the component σ_x is maximized at 80 min. Then, the sign change of the slope implies the recovery of residual stresses. The same figure shows that the component σ_y relaxes completely in 80 min, which corroborates the results obtained by Fernández *et al*. (2005) from a similar alloy. In addition, the less compressive principal component σ_q also relaxes completely in 80 min (Fig. 4b). All directions relaxed completely in 80 min are shown in Fig. 9. These are near the axis y. It is noteworthy that the y direction is perpendicular to the rolling direction where the accumulated plastic strain introduced via rolling is minimal. Along all other directions, the stress relaxation is not complete at 80 min and it is not longer possible further relaxation. On the contrary, in these directions small compressive residual stresses are also recovered. This recovery process occurs after 80 min to rearrange and match the residual stress levels relaxed in all directions. This takes place in order to minimize the total strain energy of the material.

In the present study, the relaxation mechanics can be explained from two phases clearly defined. After 20 min, the stress relaxation progresses in all directions, with normal components varying linearly. Then, the relaxation is completed in some preferential directions (Fig. 9). This fact leads to the end of the relaxation phase for all in-plane directions. This process takes about 80 min. Afterward, a recovery phase begins. This second phase takes 20 min. It is important to note that, in the second phase, small residual stresses are retrieved in the directions which are not relaxed completely. The maximum value (-10.2 MPa) corresponds to the σ_p

component. This result was expected because at 80 min the more compressive principal direction is very close to the rolling direction (*x* axis), in which the accumulated plastic strain introduced by rolling is maximized. In different directions, small residual stress recovery cease when the normal components approach the values corresponding to the directions relaxed completely. Therefore, the values relaxed at the end of the recovery phase will be similar for all in-plane directions (quasi-isotropic state). Finally, the normal stress amplitude corresponding to these values, as is shown in the smallest Mohr's circle in Fig. 5b, is -33±0.7 MPa.

CONCLUSION

A micro-indent method has been adapted to determine with high accuracy normal and tangential components of residual stress, which were relaxed in aluminium alloy specimens subjected to thermal loadings. By implementing different thermal treatments, the residual stress relaxation process was studied in these specimens at different times. An innovative data analysis using Mohr's circles allowed evaluating the relaxation mechanics in all directions of the in-plane residual stress field. The relaxation phase could only be active when the relief was possible in all directions. The normal components of residual stress were relieved following a linear pattern in time. The maximum levels were detected in directions very near to the rolling direction where the accumulated plastic strain introduced via rolling was maximized. The relaxation phase finished when the relief was completed in some preferential directions near to the axis *y*, which is perpendicular to the rolling direction. After the relaxation phase, a recovery process was activated in the material to equal the values of the normal components relaxed in all directions. Finally, the rolling direction was not relevant during this last phase.

ACKNOWLEDGMENT

The authors acknowledge the financial support of Universidad Tecnológica Nacional and Consejo Nacional de Investigaciones Científicas y Técnicas of Argentina.

REFERENCES

Allen, A.J., M.T. Hutchings, C.G. Windsor and C. Andreani, 1985. Neutron diffraction methods for the study of residual stress fields. Adv. Phys., 34(4): 445-473.

Ashby, M.F., 1972. A first report on deformation-mechanism maps. Acta Metall., 20(7): 887-897.

Benedetti, M., V. Fontanari and B.D. Monelli, 2010. Plain fatigue resistance of shot peened high strength aluminium alloys: Effect of loading ratio. Proc. Eng., 2(1): 397-406.

Bevington, P.R. and D.K. Robinson, 2003. Data Reduction and Error Analysis for the Physical Sciences. 3rd Edn., McGraw-Hill, Boston.

Bruin, W.D., 1982. Dimensional stability of materials for metrological and structural applications. CIRP Annals, 31(2): 553-560.

Busch, T., R. Harlow and R.L. Thompson, 1998. Fundamentals of Dimensional Metrology. Delmar Publishers, Albany, NY.

Das, S. and U. Chandra, 2003. Residual Stress and Distortion. In: Totten, G.E. and D.S. Mac Kenzie (Eds.), Handbook of Aluminum. Vol. 1, Physical Metallurgy and Processes. Marcel Dekker Inc., New York, pp: 305-349.

Dean, J., G. Aldrich-Smith and T.W. Clyne, 2011. Use of nanoindentation to measure residual stresses in surface layers. Acta Mater., 59(7): 2749-2761.

Díaz, F.V., G.H. Kaufmann and O. Möller, 2001. Residual stress determination using blind-hole drilling and digital speckle pattern interferometry with automated data processing. Exp. Mech., 41(4): 319-323.

Díaz, F.V., R.E. Bolmaro, A.P.M. Guidobono and E.F. Girini, 2010. Determination of residual stresses in high speed milled aluminium alloys using a method of indent pairs. Exp. Mech., 50(2): 205-215.

Díaz, F.V., C.A. Mammana and A.P.M. Guidobono, 2015. Evaluation of residual stresses in low, medium and high speed milling. Res. J. Appl. Sci. Eng. Technol., 11: 252-258.

Farago, F.T. and M.A. Curtis, 1994. Handbook of Dimensional Measurement. 3rd Edn., Industrial Press Inc., New York.

Fernández, P., R. Fernández, G. González-Doncel and G. Bruno, 2005. Correlation between matrix residual stress and composite yield strength in PM 6061Al–15 vol% SiCw. Scripta. Mater., 52(8): 793-797.

Gere, J.M., 2001. Mechanics of Materials. 5th Edn., Brooks/Cole, Pacific Grove, CA.

Gupta, B.P., 1973. Hole-drilling technique: Modifications in the analysis of residual stresses. Exp. Mech., 13(1): 45-48.

Hearn, E.J., 1997. Mechanics of Materials. Butterworth/Heinmann, Oxford.

Juijerm, P., I. Altenberger and B. Scholtes, 2007. Influence of ageing on cyclic deformation behavior and residual stress relaxation of deep rolled as-quenched aluminium alloy AA6110. Int. J. Fatigue, 29(7): 1374-1382.

Lu, J., 1996. Handbook of Measurement of Residual Stresses. Fairmont Press Inc., Lilburn, GA.

Luan, W., C. Jiang and V. Ji, 2009. Thermal relaxation of residual stresses in shot peened surface layer on TiB2/Al composite at elevated temperatures. Mater. Trans., 50(6): 1499-1501.

Noyan, I.C. and J.B. Cohen, 1987. Residual Stress: Measurement by Diffraction and Interpretation. Springer-Verlag, New York.

Prevéy, P.S., 1986. X-Ray Diffraction Residual Stress Techniques. Metals Handbook, Vol. 10, American Society for Metals, Metal Park, OH, pp: 380-392.

Rendler, N.J. and I. Vigness, 1966. Hole-drilling strain-gage method of measuring residual stresses. Exp. Mech., 6(12): 577-586.

Schoeck, G., 1961. Theories of Creep. In: Dorn, J.E. (Ed.), Mechanical Behavior of Materials at Elevated Temperatures. McGraw-Hill Book Company Inc., New York, pp: 79-107.

Seifi, R. and D. Salimi-Majd, 2012. Effects of plasticity on residual stresses measurement by hole drilling method. Mech. Mater., 53: 72-79.

Suresh, S. and A.E. Giannakopoulos, 1998. A new method for estimating residual stresses by instrumented sharp indentation. Acta Mater., 46(16): 5755-5767.

Timoshenko, S.P. and J. Goodier, 1970. Theory of Elasticity. McGraw-Hill, New York.

Tiryakioğlu, M. and J.T. Staley, 2003. Physical Metallurgy and the Effect of Alloying Additions in Aluminum Alloys. In: Totten, G.E. and D.S. Mac Kenzie (Eds.), Handbook of Aluminum. Vol. 1, Physical Metallurgy and Processes. Marcel Dekker Inc., New York, pp: 81-209.

Van Boven, G., W. Chen and R. Rogge, 2007. The role of residual stress in neutral ph stress corrosion cracking of pipeline steels. Part I: Pitting and cracking occurrence. Acta Mater., 55(1): 29-42.

Withers, P.J. and H.K.D.H. Bhadeshia, 2001. Residual stress. Part 1 – Measurement techniques. Mater. Sci. Technol., 17(4): 355-365.

Wyatt, J.E. and J.T. Berry, 2006. A new technique for the determination of superficial residual stresses associated with machining and other manufacturing processes. J. Mater. Process. Tech., 171(1): 132-140.